Materials and Design 63 (2014) 552–564

Contents lists available at ScienceDirect

Materials and Design

journal homepage: www.elsevier.com/locate/matdes

On dynamic deformation behavior of WE43 magnesium alloy sheet under shock loading conditions

H. Asgari *, A.G. Odeshi, J.A. Szpunar

Department of Mechanical Engineering, University of Saskatchewan, Saskatoon, Canada

ARTICLE INFO

Article history:
Received 27 April 2014
Accepted 16 June 2014
Available online 3 July 2014

Keywords:
Magnesium alloy sheet
Anisotropy
Twinning
Texture evolution

ABSTRACT

In the present study, the texture evolution, microstructure and mechanical behavior of WE43 magnesium sheet at high strain rates are investigated. Samples cut along the rolling direction (RD), 45° from the RD, transverse direction (TD) and perpendicular to the RD-TD plane were tested at strain rates of 800, 1200 and 1400 s^{-1} using Split Hopkinson Pressure Bar. It is observed that after shock loading, the initial weak texture converts to a weak (00.2) basal texture in all samples. Besides, it is found that the strength and ductility increase and twinning fraction decreases with increase in strain rate. Moreover, another effect of increase in strain rate is found to be the higher activation of pyramidal $\langle c+a \rangle$ slip systems. In addition, degree of stress and strain anisotropy is low particularly at higher strain rates, which is mainly related to the weak initial texture of the samples. A viscoplastic self-consistent model with a tangent approach is used to analyze the deformation mechanism during shock loading.

1. Introduction

Magnesium alloys are excellent candidates for several structural applications in the automotive and aerospace industries because of their high strength-to-density ratio, good machinability and weldability. Using magnesium alloys, it is possible to design lighter structural components which give rise to improved fuel efficiency of vehicles and airplanes and reduced greenhouse gas emission [1–3]. Unfortunately, wide industrial applications of magnesium are limited because of poor ductility at room temperature and a strong basal texture of magnesium sheets in which most of the grains are oriented with their basal poles perpendicular to the sheet plane [1–3]. Considering the intrinsic plastic anisotropy of the HCP crystals, such a texture is unfavorable for rolling operations and formability decreases [1–3]. In addition, in HCP lattice of magnesium, there is not sufficient number of active slip systems to satisfy von Mises criterion in which at least five independent slip systems are required in each grain to accommodate any arbitrary homogeneous deformation of polycrystalline materials [1–3]. The common method to improve the formability of magnesium alloys is to form the alloy at elevated temperature. However, this consumes a lot of energy which leads to a significant increase in production cost [1–3].

A suitable way to increase the ductility of magnesium wrought products would be the development of a more random grain orientation or weaker texture. It has been shown in a number of studies that the addition of rare earth (RE) elements can significantly improve the ductility due to texture modification [4–6]. The addition of rare earth elements such as yttrium, neodymium and cerium will lead to a weaker or random texture during rolling operation, resulting in improved ductility of magnesium alloys [4–6]. Also, the addition of RE elements promotes the activation of $\langle c+a \rangle$ pyramidal slip at room temperature that gives rise to better ductility [4,5,7].

In some structural applications, components are subjected to a wide range of strain rates. For instance, the mechanical behavior at high strain rates is of great interest for automotive and aerospace industries because some critical components must be able to show adequate damage resistance under severe loading conditions such as car crash or bird strike in airplanes [8]. Also, considering the fact that the deformation behavior of wrought magnesium alloys is highly dependent on the initial texture, it is very important to evaluate and understand the dynamic mechanical response of magnesium alloys to impact loading.

To date, unfortunately, a limited literature is available on the texture evolution, microstructural development, deformation mechanisms and dynamic mechanical behavior of rare-earth (RE) containing wrought magnesium alloys sheet, such as WE43, at high strain rate compressive loading. For instance, in a research conducted by Hamilton et al., only the microstructure of cast WE43

* Corresponding author. Tel.: +1 3063614637; fax: +1 3069665427.
E-mail addresses: hamed.asgari@usask.ca, asgari.ha@gmail.com (H. Asgari).

http://dx.doi.org/10.1016/j.matdes.2014.06.038
0261-3069/

alloy was investigated at high strain rate compressive loadings to check the shear localization and the texture evolution, mechanical properties and also simulation of results were not performed to establish a strong relationship between the texture, microstructure, deformation mechanisms and mechanical properties [9]. Furthermore, in another research, the tensile shock loading tests were conducted on extruded WE43 to investigate the texture evolution and mechanical properties without enough focusing on the microstructural changes after shock loading [10]. Therefore, the main objective of the present study is to investigate the texture evolution, microstructural development, deformation mechanisms and anisotropy of mechanical behavior of WE43 magnesium alloy sheet under dynamic compressive shock loading conditions. A complete, comprehensive and related series of information including texture evolution, microstructural development and mechanical properties at compressive shock loading will be presented in this paper. Besides, deformation mechanisms involved in shock loading deformation will be discussed using both experimental and simulated results.

2. Experimental procedure

The as-rolled sheet used in this study was hot-rolled WE43 magnesium alloy sheets, and its nominal chemical composition is given in Table 1. The mechanical behavior of the samples in compression under shock loading conditions was investigated using Split Hopkinson Pressure Bar (SHPB) at strain rates of 800, 1200 and 1400 s^{-1}. Four groups of samples (Fig. 1) were used for shock loading experiments; they were cut in the rolling direction (RD, 0°, hereafter denoted as IP0), in 45° to the RD (hereafter denoted as IP45), in the transverse direction (TD, 90°, hereafter denoted as IP90) and in the direction perpendicular to the RD-TD plane (hereafter denoted as OP). The shock loading samples were machined from the hot-rolled plate into cylindrical shaped samples and all samples had the same height of 10.5 mm and diameter of 9.5 mm. Direction of compression was parallel to the longitudinal direction of all cylindrical samples (Fig. 1). The sample ends were lubricated to eliminate the friction effect during impact. It should be mentioned that to check the repeatability of the results, three tests were conducted under each set of conditions and the averages of the results were reported. The variation in stress was generally less than 5%.

The texture of the samples, before and after shock loading, was measured using X-ray diffraction (XRD). The compression plane, i.e. the plane which was perpendicular to the compression direction, was considered for texture measurements in all samples (e.g. 'RD-TD' plane for OP sample, 'TD-ND' for IP0, 'RD-ND' for IP90 and 'ND-DRD' for IP45. "DRD" was selected as an arbitrary direction (45° to RD). The X-ray diffraction (XRD) experiments were done using Bruker D8 discover diffractometer with Cu Kα radiation and VANTEC 500 area detector. Furthermore, six incomplete pole figures (PF), namely (10.0), (00.2), (10.1), (10.2), (11.0) and (10.3) were determined and (00.2) and (10.0) pole figures were presented. Using incomplete pole figures, orientation distribution function (ODF) was determined by ResMat software. Finally, inverse pole figures (IPF) were plotted.

For characterization of the samples' microstructure, a field emission scanning electron microscope Hitachi SU6600 FE-SEM

Table 1
Chemical composition (in wt.%) of the WE43 alloy.

Mg	Li	Mn	Nd	Y	Zn	Zr	RE[a]
Bal.	0.05	0.03	2–2.5	3.7–4.3	0.06	0.2–1	0.3–1

[a] Other rare earth (RE) elements including Gd, Dy, Er, Sm and Yb.

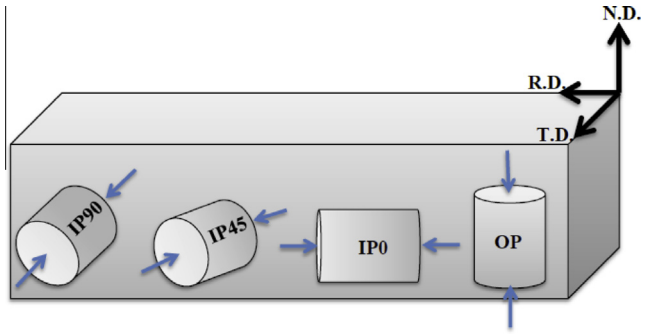

Fig. 1. Schematic diagram of the samples and compression directions (thin blue arrows). (For interpretation of the references to color in this figure legend, the reader is referred to the web version of this article.)

was used. Orientation Imaging Microscopy (OIM) was utilized to study grain orientation and twinning via electron backscattered diffraction (EBSD) by a Hitachi SU6600 FE-SEM fitted with Oxford Instruments. Data analysis was carried out using (hkl) Channel 5 data acquisition and analysis software.

To prepare for scanning electron microscopy (SEM) and orientation imaging microscopy (OIM), the samples were polished with 2000 and 4000 SiC papers followed by 3, 1 and 0.25 μm alcohol-based diamond suspensions. The final step of polishing was done using colloidal silica solution (0.04 μm) that was mixed with ethanol and ethylene glycol. To avoid corrosion or oxidation of the samples, in all the grinding and polishing steps pure ethanol was used to wash and clean the samples. To analyze the microstructure using SEM, an acetic-glycol etchant (20 ml acetic acid, 1 ml nitric acid, 60 ml ethylene glycol and 20 ml water) was used for about 10 s to reveal the grain boundaries and twins in the samples.

In order to discuss the mechanism of texture formation, numerical simulation of the texture formation was performed using VPSC-7 (Visco-Plastic Self-Consistent-7) developed by Lebensohn and Tome [11]. The applied ratios of critical resolved shear stress (CRSS) are listed in Tables 2 and 3. It should be mentioned that in the calculations, the initial texture is represented by 2000 grains representing the same volume fraction as the measured texture. Besides, we assumed a simplified linear hardening for all slip systems and extension twinning which is given as:

$$\hat{\tau}^s = \tau_0^s + \theta^s \Gamma,$$

$$\Gamma = \Sigma_s \gamma^s \tag{1}$$

where θ^s and τ_0^s are the shear strain hardening rate and the initial threshold stress for the shear system s. Also, γ^s is the accumulated

Table 2
Shear systems and their properties used in the simulations.

Basal (0001)⟨2−1−10⟩		Pyramidal ⟨c + a⟩ {10−11}⟨−12−10⟩	Extension twinning {10−12}⟨−1011⟩
τ_0	1	8	2
θ	10	10	10

Table 3
Shear systems and their properties used in the simulations (higher strain rates).

Basal (0001)⟨2−1−10⟩		Pyramidal ⟨c + a⟩ {10−11}⟨−12−10⟩	Extension Twinning {10−12}⟨−1011⟩
τ_0	1	7	2
θ	10	10	10